Extremophiles (2018) 22:447–459
https://doi.org/10.1007/s00792-018-1007-x

ORIGINAL PAPER

Shifts of methanogenic communities in response to permafrost thaw results in rising methane emissions and soil property changes

Shiping Wei[1,2] · Hongpeng Cui[1] · Youhai Zhu[3] · Zhenquan Lu[3] · Shouji Pang[3] · Shuai Zhang[3] · Hailiang Dong[1] · Xin Su[1,2]

Received: 23 August 2017 / Accepted: 5 February 2018 / Published online: 10 February 2018

Abstract

Permafrost thaw can bring negative consequences in terms of ecosystems, resulting in permafrost collapse, waterlogging, thermokarst lake development, and species composition changes. Little is known about how permafrost thaw influences microbial community shifts and their activities. Here, we show that the dominant archaeal community shifts from *Methanomicrobiales* to *Methanosarcinales* in response to the permafrost thaw, and the increase in methane emission is found to be associated with the methanogenic archaea, which rapidly bloom with nearly tenfold increase in total number. The *mcrA* gene clone libraries analyses indicate that *Methanocellales*/Rice Cluster I was predominant both in the original permafrost and in the thawed permafrost. However, only species belonging to *Methanosarcinales* showed higher transcriptional activities in the thawed permafrost, indicating a shift of methanogens from hydrogenotrophic to partly acetoclastic methane-generating metabolic processes. In addition, data also show the soil texture and features change as a result of microbial reproduction and activity induced by this permafrost thaw. Those data indicate that microbial ecology under warming permafrost has potential impacts on ecosystem and methane emissions.

Keywords Archaea community · Methanogenic community · Permafrost thaw · Methane emission · *mcrA*

Introduction

Permafrost, covering approximately 25% of the land surface on Earth, comprises a vast terrestrial ecosystem in the cold regions and is quite vulnerable to climate change (Anisimov and Nelson 1996; McGuire et al. 2009; Schuur et al. 2008; Zhang et al. 1999). With global warming, it has been estimated that as much as 90% of the permafrost will be lost by the year of 2100 (Lawrence and Slater 2005). Permafrost thawing can trigger permafrost collapse, waterlogging, thermokarst development, followed by a complete change in soil structure, as well as ecological succession and many other ecosystem changes. Among these changes, permafrost thawing elicits grave concern about the fate of the immense amount of organic carbon stored in permafrost (Anthony et al. 2014; Schuur et al. 2008; Allison and Treseder 2011). The rising temperatures will promote the metabolic rates of indigenous microbial decomposers, which will have more organic carbon due to the permafrost melting (Schuur et al. 2008; Mackelprang et al. 2011), thus making the permafrost ecosystem a significant natural source of methane, which acts as a positive feedback to accelerate climate warming (Wagner et al. 2003; Smith et al. 2004; Anthony et al. 2014).

Permafrost thaw has the potential to significantly change the permafrost ecosystem structures and functions by deepening the active layer, changing the landscape features, altering soil moisture and nutrient content, influencing species

Communicated by A. Oren.

Electronic supplementary material The online version of this article (https://doi.org/10.1007/s00792-018-1007-x) contains supplementary material, which is available to authorized users.

✉ Shiping Wei
weishiping@cugb.edu.cn

✉ Xin Su
xsu@cugb.edu.cn

[1] State Key Laboratory of Biogeology and Environmental Geology, China University of Geosciences, Beijing 100083, China

[2] School of Marine Sciences, China University of Geosciences, Beijing 100083, China

[3] Oil and Gas Survey, Geological Survey, Beijing 100029, China

composition, and ultimately shifting the permafrost ecosystem from carbon sink to carbon source (Vitt et al. 2000; Christensen et al. 2004; Schuur et al. 2008; Yang et al. 2010a, b; Allison and Treseder 2011; Jansson and Tas 2014). In upland ecosystems, permafrost thaw resulted in frequently observed polygonal patterns of troughs and pits (Osterkamp et al. 2000), and a vegetative transition from hygrophilous community to xeromorphic or shrub community (Sturn et al. 2001; Chapin et al. 2005). In lowland ice-rich ecosystems, permafrost thaw often caused transitions from permafrost ecosystems to aquatic ecosystems or wetlands (Woo 1992; Osterkamp et al. 2000), and an aquatic grass and plant community may become established. In contrast, possible microbial community responses to permafrost thaw remain largely uncertain (Allison and Treseder 2011; Graham et al. 2012; Jansson and Tas 2014).

Microbial community composition along a permafrost thaw gradient in northern Sweden revealed that diversity and abundance of methanogens were different among palsa frozen, bog thawing, and fen thawed environments. In thawing permafrost, *Candidatus Methanoflorens stordalenmirensis* was present in high abundance and was identified as a major contributor to global methane production (Mondav et al. 2014). To characterize the microbial response to permafrost thaw, a short-term thaw experiment's results indicated a rapid microbial community change during the transition from a frozen to thawed permafrost, and functional genes involved in cycling of C and N shifted in abundance during permafrost thaw (Mackelprang et al. 2011). Permafrost microbial communities usually show a lower general functional gene transcription compared to communities in the thawed soils (Hultman et al. 2015). The low temperature and limited water and solutes are thought to be constraints upon microbial activity (Steven et al. 2006; Allison and Treseder 2011; Jansson and Tas 2014). Global warming leads to permafrost thaw, which allows the organic matter within the permafrost to be released to active layers. It was estimated that there are 1,672 Pg of organic carbon stored in permafrost, which is approximately equal to the total amount of organic carbon in terrestrial vegetation and the atmosphere (Graham et al. 2012). Permafrost thaw also leads increased microbial activities (Mackelprang et al. 2011; Hultman et al. 2015), thus making more released organic carbon accessible for microbial decomposition (Schuur et al. 2009; Mackelprang et al. 2011; Graham et al. 2012), which is the dominant pathway of soil organic carbon feedback from terrestrial ecosystems to the atmosphere (Schuur et al. 2008). Permafrost thaw and the resulting release of greenhouse gases from decomposing soil organic carbon make the permafrost a significant natural source of methane having the potential to accelerate climate warming (Wagner et al. 2003; Smith et al. 2004). In permafrost soils, methane is primarily produced by obligate anaerobic methanogens, which specifically use methyl coenzyme M reductase (MCR), encoded by *mcr* genes (*mcrA*, *mcrB,* and *mcrG*) to catalyze the terminal step in biogenic methane production (Hallam et al. 2003). With permafrost melting under warmer conditions, the previous constraints of temperature, water, and nutrients will be eliminated, resulting in elevated functional gene activities for biogenic methane emission feeding back to climate change (Mackelprang et al. 2011; Mondav et al. 2014; Hultman et al. 2015).

The alpine permafrost on the Qinghai–Tibetan Plateau is the largest permafrost region on Earth, occupying an estimated of 1.5×10^6 km^2 and accounting for about one-sixth of China's land area (Jin et al. 2000). This alpine permafrost has been experiencing degradation from climate warming (Yang et al. 2010a, b). During the thaw, microbial action mobilized the stored carbon in the permafrost, resulting in greenhouse gas emissions. It was estimated that the annual methane emissions are about 0.7–0.9 Tg from the cold wetlands of the Qinghai–Tibetan Plateau (Jin et al. 1999). Despite the previous advances in studies of permafrost microbial diversity and composition, their responses to permafrost thaw remain unclear. In this study, we collected permafrost soil samples from Qinghai–Tibetan Plateau and used cultured strategy to ascertain the archaeal and methanogenic community changes in response to permafrost thaw, and in turn, elucidate the effects of rising temperatures and microbial activity feedbacks on methane emissions and soil environments.

Materials and methods

Study site and sampling

The sampling site (N38°05′38.10″ and E99°10′05.13″) is located in Qinghai–Tibetan Plateau, which has the largest alpine permafrost area on Earth. The mean annual ground temperature of the study area is approximately − 2.4 °C with an altitude of 4,000–4,300 m, with the plateau's precipitation occurring mainly in summer to give a natural ecosystem of alpine swamp meadows. The vegetation of the study area is covered predominantly by *Kobresia humilis* and *Carex moorcroftii*. The active layer of the permafrost, with the thickness varying from 20 to 60 cm, thaws every summer and completely freezes during the winter. Data from wireline logging indicate the thickness of permafrost ranges from 65–95 m, and may exceed 100 m in large parts of this region (Wang et al. 2014).

Samples were collected being obtained by digging to a depth of 1.6 m. Samples for both soil characteristic analysis and incubation experiment were taken aseptically from a depth of 1.5 m, which was still frozen up to the depth of 55 cm. The soil samples were placed into sterilized plastic

bags for soil texture and features analyses and into 50-ml centrifuge tubes for microbiological analyses. All the samples were kept frozen in insulated containers and transported immediately to laboratory for further analyses.

Soil characteristic techniques

The soil characteristic techniques were adopted as Wei et al. (2014) described, with modifications. The pH of soil was determined using a fresh soil to water ratio of 1:5 (pH meter, Sartorius PB-10). Total soil carbon content was determined by combustion for 16 h at 375 °C. The original soil methane concentration was obtained by thawing 10-g soil into a 50-ml bottle containing 20 ml of saturated NaCl solution. Ten milliliters of headspace were taken from the bottles for methane measurement by gas chromatography using a Packard Model 438A fitted with a flame ionization detector. Acetate content was measured by HPLC as described by Metje and Frenzel (2005). The soil texture before and after incubation was analyzed by determining the proportion of sand, silt, and clay particles in the soil. Forty grams of air dried (crushed to < 2 mm) soil was shaken for 16 h with 100 ml of 5% sodium hexametaphosphate. The suspension was stirred vigorously for 1 min to suspend the particles. An ASTM No. 152H hydrometer was carefully placed in the suspension and used to take two readings. The percentage of sand, silt, and clay in the soil was calculated from the resulting hydrometer readings.

X-ray powder diffraction (XRD) was used to determine the mineralogy of the soil. The soils before and after incubation were dried and ground into fine powder of size of less than 10 μm (or 200-mesh). The powdered sample was back-packed into an aluminum sample holder and made its surface was flattened, and then was analyzed using XRD on a Panalytical X'Pert PRO MPD (Cu-Kα). Instrument parameters were set to 30-kV accelerating voltage and 10-mA current. Scans were run from 5° to 60° 2θ at a scanning speed of 0.3°/s.

Incubation experiment

For incubation experiments, triplicate soil samples were collected on site. Approximately 25 g of frozen soil was placed in 250-ml glass bottles and immediately flushed with N_2 for 5 min, then sealed with rubber stoppers, and shipped to the laboratory for incubation. The bottles with samples were incubated at 15 °C for 21 days in the dark. Ten milliliters of headspace were taken from the bottles for methane measurement by gas chromatography using a Packard Model 438A fitted with a flame ionization detector. After the incubation, the samples were subjected to soil characteristic analyses including pH, TOC, grain size, XRD, and microbial analyses including gene copy numbers of archaeal 16S rRNA, *mcrA*, and the communities of archaea and methanogens.

Nucleic acids extraction and RNA reverse transcription

Total genomic DNA and RNA were extracted from 2-g soil of each sample using the FastDNA® SPIN Kit for Soil (MP) and the RNA Powersoil Total RNA Isolation Kit (MoBio) following the manufacturer's instructions. The extracted RNA was treated with RQ1 RNase-Free DNase (Promega) according to the manufacturer's protocol. Reverse transcription was carried out on total RNA using SuperScript III (Invitrogen) and random hexamers, following the manufacturer's instructions.

PCR and quantitative PCR

Archaeal 16S rRNA genes were PCR amplified from the total DNA extracted from soil with the primers Arch21F (5′TTCCGGTTGATCCYGCCGGA) and Arch958R (5′YCC GGCGTTGAMTCCAATT) (DeLong 1992). *mcrA* genes were PCR amplified with the primers *mcrA*F (5′GGTGGT GTMGGATTCACACARTAYGCWACAGC) and *mcrA*R (5′TTCATTGCRTAGTTWGGRTAGTT) from the soil total DNA and the reverse transcribed RNA, respectively (Luton et al. 2002). The PCR reaction volumes for both target genes were identical. The 50-μl reaction mixtures were composed of 0.25-μM each primer, 0.2-mM dNTPs, 1.5-mM $MgCl_2$, 5 μl of Taq buffer, and 5-U Taq DNA polymerase (Invitrogen, USA); 20-ng template DNA. PCR amplifications were carried out with 1 min at 95 °C, 30 cycles of 1 min at 94 °C, 1 min at 50 °C for archaeal 16S rRNA gene amplification or 1 min at 55 °C for *mcrA* gene amplification, and 1.5 min at 72 °C, followed by a final extension step of 10 min at 72 °C.

Archaeal 16S rRNA genes and *mcrA* genes of methanogenic archaea were subjected to quantitative PCR (qPCR) analyses. The qPCR primers were Arch349F (59′GYG-CASCAGKCGMGAAW-39) and Arch806R (5′GGACTA CVSGGGTATCTAAT) for archaeal 16S rRNA genes (Takai and Horikoshi, 2000), and ME3MF (5′TGTCNG-GTGGHGTMGGSTTYAC) and ME2r' (5′TCATBGCR TAGTTDGGRTAGT) for *mcrA* genes (Hales et al. 1996; Nunoura et al. 2008). qPCR amplification was performed using an ABI prism 7500 sequence detection system (Applied Biosystems, USA), and all the reactions were in a volume of 25 μl containing 10 ng of template DNA, 12.5 μl of SYBRGreen mastermix (Applied Biosystem, USA), and 4.5 μl each of forward and reverse primers. The qPCR amplification for *mcrA* genes consisted of 1 cycle of 95 °C for 10 s, followed by 40 cycles of 95 °C for 45 s, 55 °C for 30 s, and extension at 72 °C for 1 min. The standards for

archaeal 16S rRNA genes were prepared from nearly full-length sequences amplified from the soil community DNA using primer sets of Arch21F/Arch958R for archaea. The standards for *mcrA* genes were prepared from *mcrA* clones amplified using primer a set of *mcrA*F/*mcrA*R.

Clone library construction and sequencing

The 16S rRNA and *mcrA* amplicons were visualized on 1% agarose gels, and purified with the PCR purification kit (TaKaRa). The purified products of 16S rRNA and mcrA were cloned into the pMD18-T vector with a TA cloning kit (TaKaRa) and transformed into of *Escherichia coli* JM109 competent cells following the manufacturer's protocol. Positive clones were randomly selected based on blue–white screening for sequencing. Sequences were determined on an ABI 3730 automated DNA sequencer (Applied Biosystems) using the archaeal primer 21f for 16S rRNA inserted clones and the universal primer M13-47 for *mcrA* inserted clones.

Phylogenetic analysis

The archaeal 16S rRNA genes and deduced amino acid sequences of *mcrA* gene were BLAST analyzed to identify their putative closest phylogenetic relatives. The sequences were aligned with their relatives using Clustal W, and phylogenetic trees for both 16S rRNA and *mcrA* genes were constructed by the neighbor-joining method using the maximum-parsimony algorithm in MEGA4 software with 1000 bootstrap replicates. Operational taxonomic units (OTUs) were determined using DOTUR program based on a cut-off value of 3% for 16S rRNA gene sequences and a cut-off value of 14.3% for McrA amino acid sequences (Schloss and Handelsman 2005; Barbier et al. 2012).

Statistical analysis

Good's coverage (C) was calculated as $[1 - (n/N)] \times 100$, where n is the number of single clone OTUs and N is the library size (Good 1953). Rarefaction curves and determination of OTU used the computer program DOTUR (Schloss and Handelsman 2005). Shannon's diversity index and Simpson's diversity index were determined using the computer program MOTHUR (Schloss et al. 2009).

Nucleotide sequence accession numbers

Nucleotide sequences of 16S rRNA gene and *mcrA* gene have been deposited in the GenBank database. The archaeal 16S rRNA gene sequences were assigned accession numbers KT964753-KT964768, and *mcrA* gene sequences were assigned accession numbers KT964743-KT964752.

Results

The predominant archaea community shifts from *Methanomicrobiales* to *Methanosarcinales*

To get insight into the community structures of archaea both in the original permafrost and in the thawed permafrost, a clone library was constructed from both types of the soil sediments. A total of 78 archaeal 16S rRNA gene sequences were retrieved from the original permafrost library (O-16S rRNA library), and they were grouped into five different operational taxonomic units (OTU) at a 97% sequence similarity threshold, whereas a total of 109 archaeal 16S rRNA gene sequences were obtained from the thawed permafrost library (I-16S rRNA library), which were assigned to 16 different OTUs. The number of clones analyzed represented 97.4 and 93.6% coverage for libraries of O-16S rRNA and I-16S rRNA, respectively (Supplementary Table S1). Sequences retrieved from both of the libraries were affiliated with two phyla, *Euryarchaeota* (97.4% of total sequences in library of O-16S rRNA compared to 93.6% of total sequences in the library of I-16S rRNA) and *Crenarchaeota* (2.6% of total sequences in library of O-16S rRNA compared to 6.4% of total sequences in the library of I-16S rRNA) (Fig. 1). The lineages of *Methanosarcinales*, *Methanomicrobiales,* and *Methanobacteriales*, affiliated with *Euryarchaeota* in the library of O-16S rRNA, accounted for 3.8, 92.3, and 1.3% of archaeal clone sequences, respectively, whereas the four lineages, *Methanosarcinales*, *Methanomicrobiales*, *Methanomassiliicoccales,* and *Methanobacteriales*, which were observed in the library of I-16S rRNA, accounting for 51.4, 36.7, 3.7, and 1.8% of the archaeal clone sequences, respectively (Fig. 1). As for the crenarchaeal sequences, only one lineage, Group 1.3b/MCG-A (Ochsenreiter et al. 2003; Meng et al. 2014; Wei et al. 2014), was detected in each clone library, which accounted for 2.6 and 6.4% of total sequences in the O-16S rRNA and I-16S rRNA libraries, respectively. The data indicated that Group 1.3b/MCG-A was a non-dominant group in the original permafrost, because even after the incubation, this group still presented a limited reproduction response to the permafrost thaw and incubation.

The relative abundance of each 16S rRNA-OTU was shown in Fig. 2a. The original permafrost was dominated by 16S rRNA-OTU1 (92.3% of total sequences) which was affiliated with *Methanomicrobiales*. However, after the permafrost thaw and incubation, the archaea community

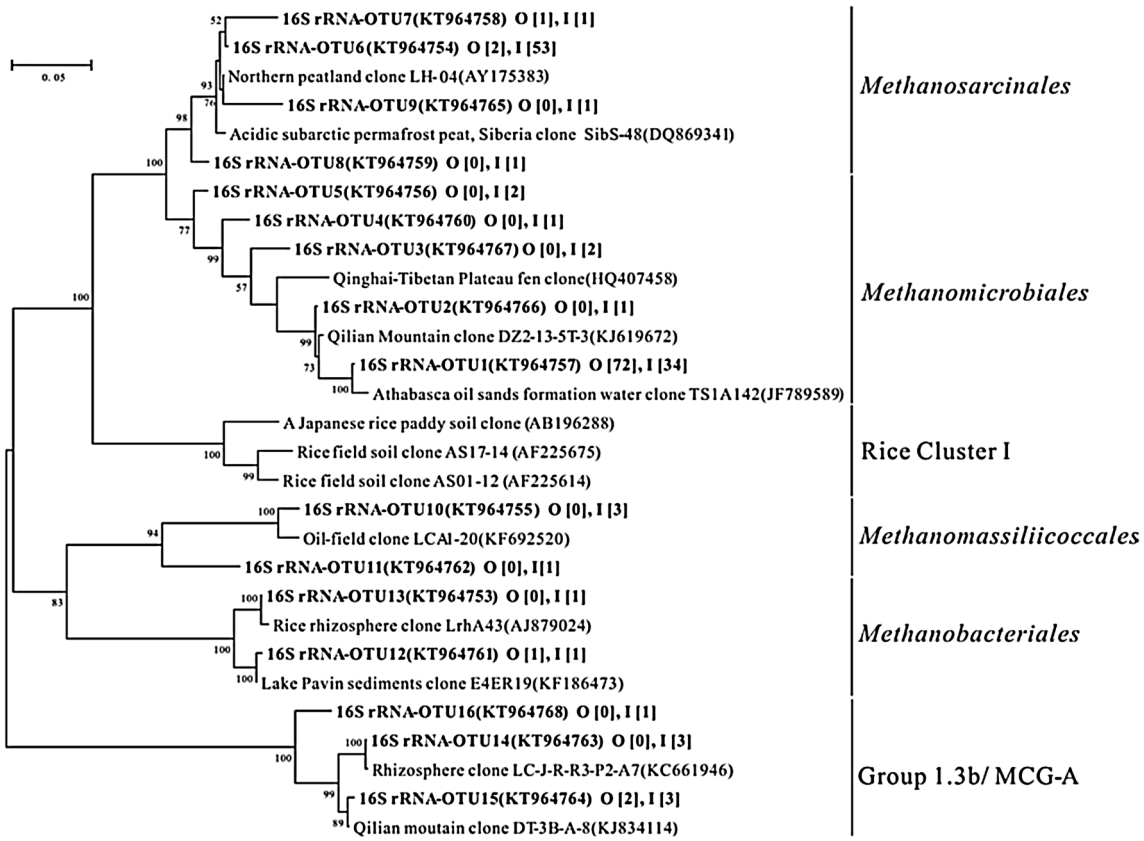

Fig. 1 Phylogenetic tree showing relationships of archaeal 16S rRNA gene sequences from the original permafrost and the incubated permafrost to reference archaeal sequences. GenBank accession numbers are given in parentheses and numbers in square brackets indicate the retrieved sequences of each OTU in their corresponding libraries (O, O-16S rRNA library; I, I-16S rRNA library). The tree was generated by neighbor-joining method. Bootstrap values are based on 1000 replicates and are shown at the nodes with greater that 50% bootstrap support. The scale bar represents a 5% nucleotide sequence divergence

was mainly composed of 16S rRNA-OTU1 (31.2% of total sequences) and 16S rRNA-OTU6 (48.6% of total sequences) which were affiliated with *Methanomicrobiales* and *Methanosarcinales*, respectively. It was clearly shown that the relative abundance of 16S rRNA-OTU1 was reduced sharply from 92.3 to 31.2%, whereas the relative abundance of 16S rRNA-OTU6 was increased significantly from 2.6 to 48.6% when comparing the communities between in the original permafrost to that of the subsequently thawed permafrost. We inferred that 16S rRNA-OTU1 was more sensitive in responding to temperature and soil environment changes. Conversely, 16S rRNA-OTU6 showed a good adaptation and a robust reproduction under the altered environmental conditions. We also noticed that more OTUs were detected in each lineage of *Methanomicrobiales*, *Methanosarcinales*, *Methanobacteriales*, and Group 1.3b/MCG-A after the permafrost thaw and incubation than in the original permafrost. Minor percentages of 16S rRNA-OTU2 to 16S rRNA-OTU5, 16S rRNA-OTU7 to 16S rRNA-OTU11, 16S rRNA-OTU13 to 16S rRNA-OTU14, and 16S rRNA-OTU16, ranging from 0.92 to 2.76%, were detected only in the thawed permafrost and not in the original permafrost, with the inferred cause being the insufficient clone sequencing depth in the original permafrost. The relative abundance of archaeal community data indicated a shift from the dominance of *Methanomicrobiales* in the original permafrost to the dominance of *Methanosarcinales* after the permafrost thawed and incubation (Fig. 2a).

Community of active methanogens shifts from *Methanocellales*/Rice Cluster I to *Methanosarcinales*

Three *mcrA* gene libraries, O-mcrA (derived from the total community DNA from the original permafrost), I-mcrA (derived from the total community DNA from the incubated permafrost), and T-mcrA (derived from the total community reverse transcribed RNA from the incubated permafrost), were constructed. A total of 3, 9, and 6 OTUs (≥ 85.7% amino acid sequence similarity) were retrieved, representing 42, 72, and 50 mcrA protein sequences with coverages

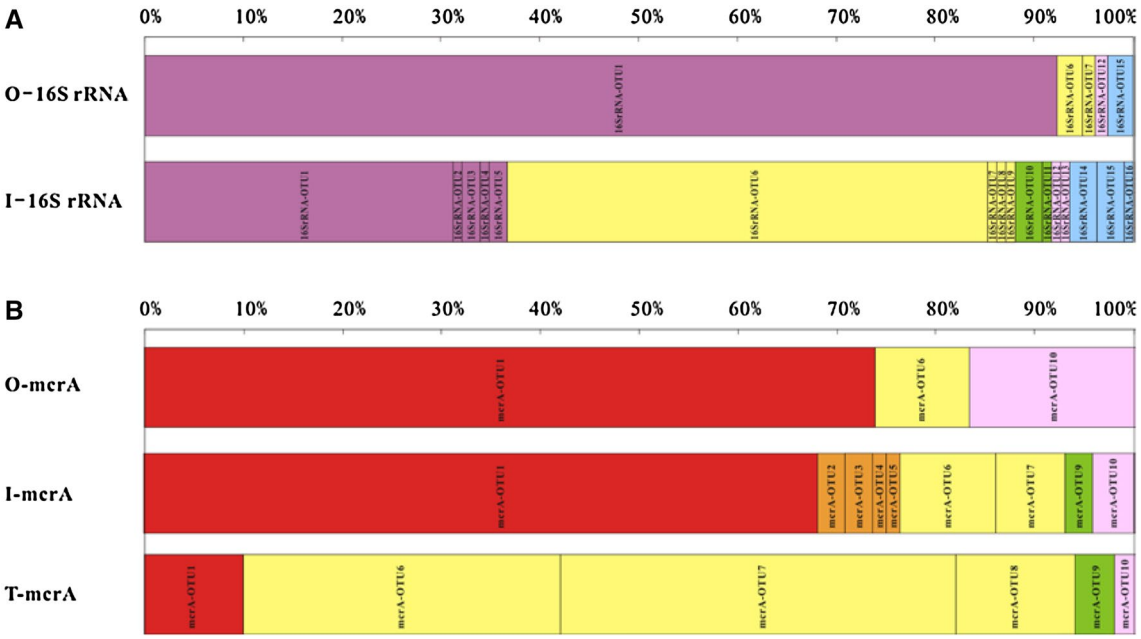

Fig. 2 Relative abundance of each OTU in the libraries. A, 16S rRNA gene libraries; B, *mcrA* gene libraries. Purple segments indicate OTUs affiliated to *Methanomicrobiales*, yellow segments indicate OTUs affiliated to *Methanosarcinales*, green segments indicate OTUs affiliated to *Methanomassiliicoccales*, pink segments indicate OTUs affiliated to *Methanobacteriales*, blue segments indicate OTUs affiliated to Group 1.3b/MCG-A, red segments indicate OTUs affiliated to Methanocellales/Rice Cluster I, and orange segments indicate OTUs affiliated to Fen Cluster

of 99.9, 97.2, and 98.0% corresponding to each library of O-mcrA, I-mcrA, and T-mcrA, respectively (Supplementary Table S1). Phylogenetic analysis of the sequences from O-mcrA library revealed that there were single OTUs affiliated with *Methanocellales*/Rice Cluster I (Sakai et al. 2008), *Methanosarcinales,* and *Methanobacteriales*, having sequence similarities of 73.8, 9.5, and 16.7% (percentage of total *mcrA* gene sequences), respectively. The library of I-mcrA was comprised of 1 OTU (68.1% of total *mcrA* gene sequences), 2 OTUs (16.7% of total *mcrA* gene sequences), 4 OTUs (8.3% of total *mcrA* gene sequences), 1 OTU (4.2% of total *mcrA* gene sequences), and 1 OTU (2.7% of total *mcrA* gene sequences), which were affiliated with *Methanocellales*, *Methanosarcinales*, Fen Cluster, *Methanobacteriales,* and *Methanomassiliicoccales*, respectively (Figs. 2b and 3). The relative abundances of OTUs occurring in each library showed that mcrA-OTU1 predominated in the libraries of both O-mcrA and I-mcrA, indicating the species belonging to mcrA-OTU1 showed adaptivity to the environmental change. It was also noticed that there were more OTUs detected in the I-16S rRNA and I-mcrA libraries than in the libraries of O-16S rRNA and O-mcrA, reflecting an insufficient clone sequencing depth both in O-16S rRNA library and in the O-mcrA library. In addition, other groups, although less prevalent than the major groups mentioned above, will also increase their absolute numbers due to their reproduction occurring during incubation.

Community composition analysis of the active functional *mcrA* gene library of T-mcrA showed that 1 OTU (10.0% of total *mcrA* gene sequences), 3 OTUs (84.0% of total *mcrA* gene sequences), 1 OTU (2.0% of total *mcrA* gene sequences), and 1 OTU (4.0% of total *mcrA* gene sequences) were affiliated with *Methanocellales*, *Methanosarcinales*, *Methanobacteriales,* and *Methanomassiliicoccales*, respectively (Figs. 2b and 3). Comparison of the relative abundance of community composition among the libraries of O-mcrA, I-mcrA, and T-mcrA clearly showed that even though the species belonging to the dominant group of *Methanocellales*/Rice Cluster I were well-adapted and reproduced, the majority of them did not undergo *mcrA* gene transcription during the permafrost thawing and incubating process. Conversely, the species belonging to the minor group of *Methanosarcinales* showed greater *mcrA* gene transcription, indicating a shift from the dominance of an inactive *mcrA* gene harboring group of *Methanocellales*/Rice Cluster I to the dominance of an activited *mcrA* gene harboring group of *Methanosarcinales* (Fig. 2b), which contribute to the biogenic methane emissions in this conditions.

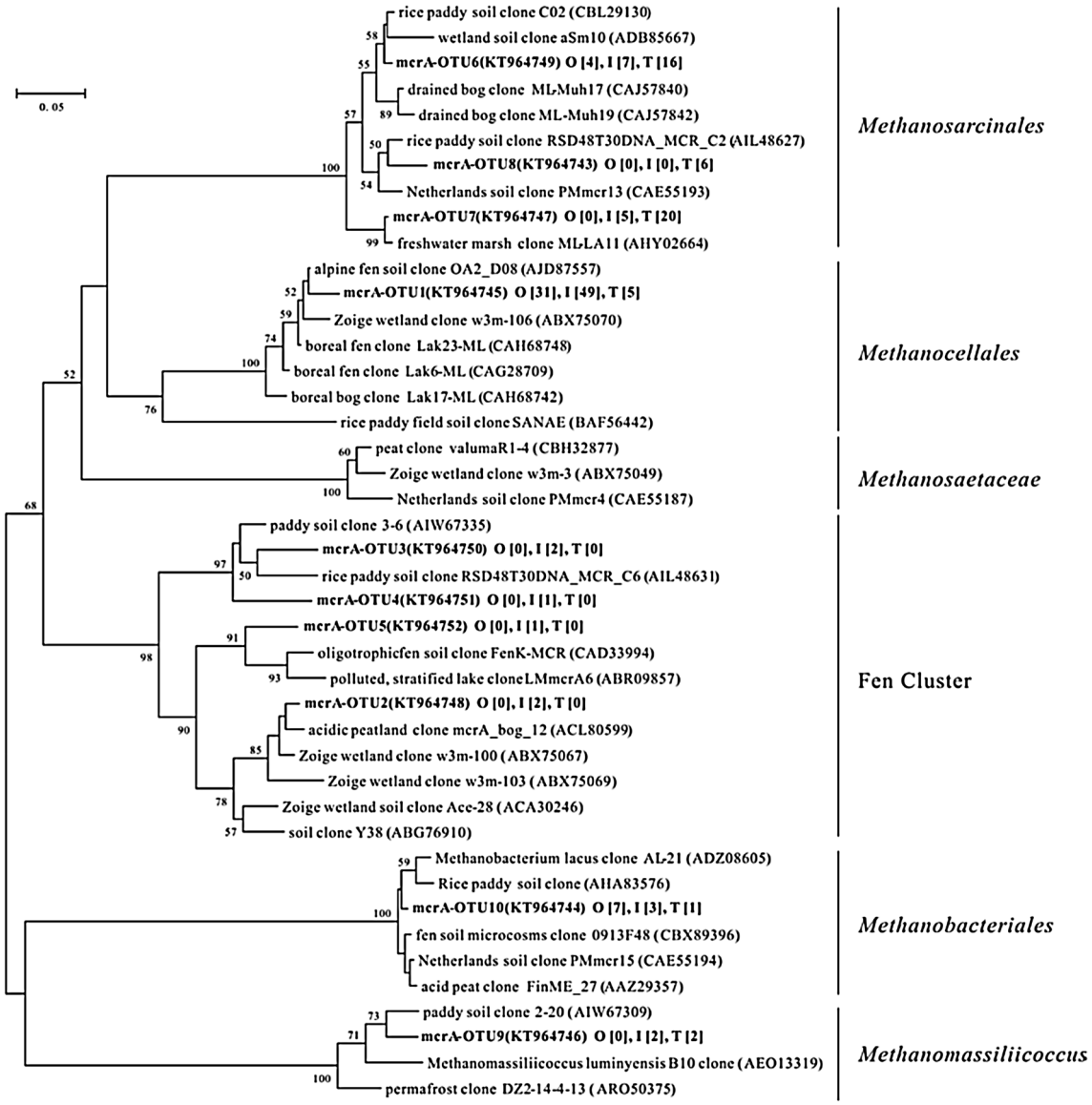

Fig. 3 Phylogenetic tree showing relationships of derived amino acid sequences encoded by *mcrA* genes to reference sequences. GenBank accession numbers are given in parentheses and numbers in square brackets indicate the retrieved sequences of each OTU in their corresponding libraries (O, O-mcrA library; I, I-mcrA library; T, T-mcrA library). The tree was generated by neighbor-joining method. Bootstrap values are based on 1000 replicates and are shown at the nodes with greater that 50% bootstrap support. The scale bar represents a 5% nucleotide sequence divergence

Methanogens bloom and transcription of the functional *mcrA* genes lead to a boost in methane emission

As the above data show, the community composition of archaea and methanogens changes during permafrost thaw and incubation. To characterize their population growth dynamics, quantitative real-time PCR was performed to determine the total archaeal 16S rRNA gene and *mcrA* gene copies in the samples. The results demonstrated that there was not much difference in the numbers of archaeal 16S rRNA gene copies between the original permafrost ($4.02 \pm 0.65 \times 10^6$ copies/g wet soil) and the thawed permafrost ($4.39 \pm 0.89 \times 10^6$ copies/g wet soil) (Fig. 4). However, numbers of the *mcrA* gene copies in both samples showed a significant increase from $6.46 \pm 1.68 \times 10^5$ copies/g wet soil to $5.50 \pm 0.71 \times 10^7$ copies/g wet soil, indicating the population of methanogens harboring *mcrA* genes bloom in response to permafrost thaw and incubation.

To determine whether *mcrA* genes were transcribed both in the original permafrost and the thawed permafrost, we

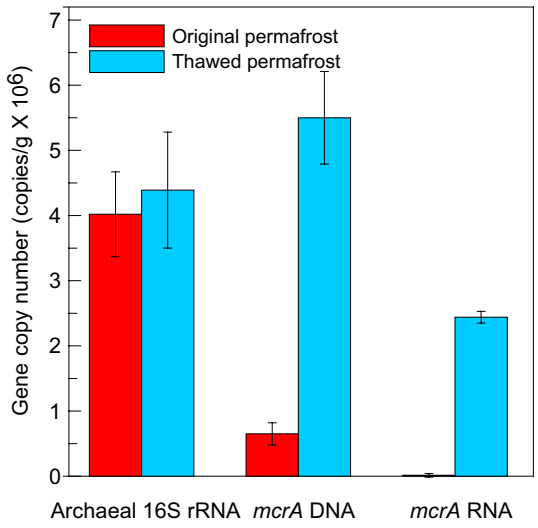

Fig. 4 Archaeal 16S rRNA and *mcrA* gene copy numbers quantified using qPCR. Error bars are means ± the standard error of three biological replicates

Fig. 5 Methane emission from original permafrost and thawed permafrost. Error bars are means ± the standard error of three biological replicates

used conventional PCR and RT-PCR to amplify the *mcrA* genes and their transcripts, respectively. Gel electrophoresis of the PCR and RT-PCR products of *mcrA* genes revealed distinct bands amplified from the total community DNA extracted from both the original permafrost and the thawed permafrost. However, there was no amplification of *mcrA* from the total community RNA, indicating that the *mcrA* genes were inactive or had very low transcriptional activity in the original permafrost. Conversely, there was an obvious amplification of *mcrA* genes from the thawed permafrost (Supplementary Fig. S1). The results of RT-qPCR suggested that *mcrA* genes coding for methanogens were transcribed at higher rates, increasing from original permafrost levels of $1.40 \pm 0.28 \times 10^4$ copies/g wet soil to thawed permafrost levels of $2.44 \pm 0.09 \times 10^6$ copies/g wet soil, which was taken for the biogenic methane production during the permafrost thaw and incubation. With elevated transcription of the functional *mcrA* genes, there were consistent increases in methane emission from 16.2 ± 2.8 ppm/g wet soil to 102.4 ± 9.4 ppm/g wet soil (Fig. 5).

Permafrost thaw feedbacks to the soil texture and features

The previous studies showed permafrost thaw in response to global warming, which results in the slumping of the soil surface and flooding. We also observed severe thermokarst failure phenomena at our sampling site in the Qinghai–Tibetan Plateau (Fig. 6). Permafrost thaw not only induces microbial community changes, but also exacerbates the greenhouse gas emission with the stored organic carbon becoming accessible to microbial decomposers through their metabolic activities. Inversely, with the permafrost thaw and activated microbial metabolic activities, the soil texture and features must undergo significant changes. To evaluate these changes, the parameters of TOC, acetate, pH, grain size, and minerals were assayed in our incubation experiment. The results showed that the soil organic carbon dropped from 15.05 ± 1.48% to 11.65 ± 0.64% (Table 1), because portion of it had been decomposed by microbes and released as methane or carbon dioxide. The acetate content, which accumulates in the soil, showed a slight increase (Table 1). Acetate is produced by other microbial organic decomposers and then utilized as the substrate for *Methanosarcinales* to generate the methane. That is likely the reason why the methanogen community shifted from *Methanocellales*/Rice Cluster I to *Methanosarcinales* after the permafrost thaw and incubation (Figs. 2b, 3). Particle size analysis revealed that the original permafrost was composed of sand (25.67%), silt (68.43%), and clay (5.94%), in comparison with the thawed permafrost's composition of sand (23.67%), silt (68.67%), and clay (7.66%). The average particle size did not change much, decreasing from 5.25 to 5.03 μm. However, in the long run, the constant deterioration of soil particles by microbes will lead to reduced aeration, which will have important effects on the soil. Soil minerals are thought to play a vital role in soil fertility. Mineral composition and semi-quantitative analysis revealed that most the minerals did not change significantly, with the original permafrost comprised of quartz (70%), feldspar (10%, plagioclase and potassium feldspar), illite (10%), chlorite (5%), and dolomite (5%), compared to the thawed permafrost composition of quartz (70%), feldspar (10%, plagioclase, and potassium feldspar), illite (10%), and chlorite (10%) (Table 1

Fig. 6 Thermokarst features of permafrost collapse in Qinghai–Tibetan Plateau

Table 1 Physical and chemical characteristics of permafrost soils

Sample	TOC (%)	Acetate (μM/g)	pH	Sand (%)	Clay (%)	Silt (%)	Minerals
Original permafrost	15.05 ± 1.48	28.6 ± 3.2	6.75 ± 0.07	25.63	68.43	5.94	Mainly quartz, minor of feldspar, illite, chlorite, dolomite
Thawed permafrost	11.65 ± 0.64	67.3 ± 5.5	6.35 ± 0.07	23.67	68.67	7.66	Mainly quartz, minor of feldspar, illite, chlorite

and Supplementary Fig. S2). The loss of dolomite mineral through decomposition was thought to be due to microbial weathering.

Discussion

Permafrost thaw resulting from climate warming was shown to cause significant ecological impacts on the permafrost landscape, soil moisture, nutrients availability, species composition, and ecosystem functions (Vitt et al. 2000; Christensen et al. 2004; Schuur et al. 2008; Yang et al. 2010a, b; Allison and Treseder 2011; Jansson and Tas 2014). However, knowledge of how the permafrost microbial community will respond to the rising temperature is still lacking. Two general strategies often employed to reveal the microbial community composition and functional gene activity shifts in response to permafrost thaw are permafrost incubation experiments or examination of the fields along the permafrost thaw (Rivkina et al. 2007; Coolen et al. 2011; Mackelprang et al. 2011; Mondav et al. 2014; Deng et al. 2015). Metagenomic analysis of a short-term incubated permafrost revealed core-specific shifts in bacterial and archaeal communities as the permafrost thawed. The archaeal communities, including *Methanosarcinales*, *Methanomicrobiales,* and *Methanobacteriales*, were detected in increasing abundance during the incubation (Mackelprang et al. 2011). However, our data showed that the original permafrost consisted of *Euryarchaeota*, including mostly *Methanomicrobiales* (92.3%) and smaller numbers of *Methanosarcinales* (3.8%) and *Methanobacteriales* (1.3%). The thawed permafrost was comprised of *Methanosarcinales* (51.4%), *Methanomicrobiales* (36.7%), *Methanomassiliicoccales* (3.7%), and *Methanobacteriales* (1.8%), indicating a clear shift of the dominant archaeal community from *Methanomicrobiales* to *Methanosarcinales* (Figs. 1, 2a). In contrast, only 2.6% of Group 1.3b/MCG-A affiliated to *Crenarchaeota* was retrieved, compared with 6.4% in the thawed permafrost, indicating *Crenarchaeota* was a non-dominant phylum in permafrost (Figs. 1, 2a). This observation is quite similar to the previous reports (Steven et al. 2008; Mackelprang et al. 2011; Wei et al. 2014). On the other hand, it also indicated that species belonging to *Crenarchaeota* had limited reproduction during the incubation. We also detected the archaeal 16S rRNA gene copies both in the original permafrost and in the thawed permafrost, with no signs of significant changes between them (Fig. 4). Coolen and co-workers (Coolen et al. 2011) were unsuccessful in amplifying the archaeal 16S rRNA genes because of their low abundance in permafrost. However, they did observe that the bacterial 16S rRNA

gene copies increased about tenfold after 11 days of incubation. Mondav et al. (2014) determined microbial community composition along a permafrost thaw gradient in northern Sweden, and observed a trend of prevalent *Methanoflorens stordalenmirensis* detected along a thaw gradient of permafrost. Deng et al. (2015) also recorded significant changes of bacterial and archaeal communities along a permafrost thaw gradient in Alaska. All the previous studies lead to the conclusion that permafrost warming and thaw will radically change the microbial community composition and cause them to bloom in abundance, thus influencing succession in the permafrost ecosystem.

Methanogenic archaea, also known as methanogens, are an important group of *Euryarchaeota* that produce methane under anaerobic conditions. They play key roles in the methane cycle of permafrost regions and consequently make significant contributions to global warming by their biogenic methane emission (Wagner et al. 2003; Wagner 2008). All known methanogens harbor the *mcrA* gene, encoding for the enzyme methyl coenzyme M reductase, which catalyzes the terminal step in biogenic methane production (Hallam et al. 2003) and makes it a suitable target for specific detection of methanogens. In this study, the methanogen communities were composed of *Methanocellales*/Rice Cluster I (73.8%), *Methanosarcinales* (9.5%) and *Methanobacteriales* (16.7%) in the original permafrost, compared to the thawed permafrost composition of *Methanocellales*/Rice Cluster I (68.1%), *Methanosarcinales* (16.7%), *Methanobacteriales* (4.2%), Fen Cluster (8.3%), and *Methanomassiliicoccales* (2.7%). The community composition was shown to not differ significantly between the original and thawed permafrost based on the taxonomic analysis at the order level. This is quite different from Mackelprang et al. (2011), in which the relative abundance of both *Methanomicrobiales* and *Methanosarcinales* were increased after the permafrost incubated for 7 days. Quantitative PCR result showed that *mcrA* gene copies in the thawed permafrost were tenfold of that in the original permafrost, indicating methanogens bloom after permafrost thaw (Fig. 4). This result was similar to that reported by Liebner et al. (2015), who studied the methanogenic community composition along the degradation of discontinuous permafrost, and found that *mcrA* gene copy numbers were increased significantly in the collapsed palsa and thermokarst pond compared to those in degrading palsa. However, Mackelprang et al. (2011) detected *mcrA* gene copy numbers through quantitative PCR and revealed that *mcrA* gene sequences did not change significantly during permafrost thaw. The transcriptional response of the microbial community in the thawed permafrost indicated that they were mostly composed of *Methanosarcinales* (84%) and *Methanomicrobiales* (10%). We did not detect any observed transcripts of *mcrA* genes in the original permafrost (Supplementary Fig. S1), indicating that transcriptional activity of *mcrA* genes was too low to be detected using the conventional RT-PCR method. According to Ernakovich and Wallenstein (2015), permafrost microorganisms are not highly functional at low temperatures, but permafrost activity and functional diversity increase with temperature elevation. Hultman et al. (2015) compared the data from metagenomic DNA and metatranscriptome RNA sequencing and found that permafrost microbial communities have a lower general functional potential than thawed soils. It is very interesting that the methanogens were dominated by Rice Cluster I in the original permafrost, which is a novel euryarchaeal lineage within the phylogenetic radiation of *Methanosarcinales* and *Methanomicrobiales* (Grosskopf et al. 1998). Previously, studies show that Rice Cluster I methanogens can convert H_2/CO_2 to CH_4. Genome data demonstrate that the enriched Rice Cluster I strain has all of the enzymes necessary for conversion of H_2 and CO_2, but lacks the acetate-activating enzymes in their genome (Conrad et al. 2006). Our data showed that the transcriptional methanogenic community was mainly classified under the order of *Methanosarcinales* as the permafrost thawed (Fig. 2). We inferred that it was related to the substrates that were available, resulting in a shift of the methanogenesis metabolic pathway. As our data show, the acetate accumulation in the thawed permafrost was higher than that in the original permafrost (Table 1). It is well known that *Methanosarcinales* are capable of using acetate as a substrate for methanogenesis (Kendall and Boone 2006), distinguishing them from *Methanomicrobiales*, which can only use H_2 and CO_2 as a substrate (Garcia et al. 2006). In a freshly thawed permafrost, Coolen and Orsi (2015) detected exclusive expression of acetogenesis transcripts, suggesting that acetogenic bacteria are a potential source of acetate for acetoclastic methanogenesis. Liebner et al. (2015) studied the methanogen community structures both in a previously collapsed palsa (CP) and in a thermokarst pond (TP), and identified a clear shift from a potentially acetoclastic members in TP to predominantly hydrogenotrophic members in CP.

Permafrost stores about 1672 Pg carbon, which is thought to be equivalent to the total amount of carbon contained within land plants and the atmosphere combined (Schuur et al. 2008; Zimov et al. 2006). This carbon pool is vulnerable to the rising temperature and faces degradation by microbial decomposers as the permafrost thaws. Microbial activities are usually constrained by the low temperatures, moisture, nutrient, and oxygen availabilities. Once the permafrost thaws, all of these constraints are removed, making the stored organic carbon more accessible for microbial decomposition, resulting in greenhouse gas emission (Schuur et al. 2008; Allison and Treseder 2011). The Qinghai–Tibetan Plateau is the largest alpine permafrost area on Earth. The previous studies estimated that the plateau contained a total of 33.52 Pg of organic carbon and that

0.7–0.9 Tg of methane were emitted annually from the plateau's grassland soils (Jin et al. 1999; Wang et al. 2002), making it a potent source of greenhouse gas emissions (Kang 1996). Our data showed that the soil organic carbon was 15.05 ± 1.48% in the original permafrost from the Qinghai–Tibetan Plateau sampling site. However, it quickly dropped to 11.65 ± 0.64% after short incubation times (Table 1), suggesting that the organic carbon was decomposed by the microbial activity and resulted in an increase in methane emission of 102.4 ± 9.4 ppm/g wet soil in the thawed permafrost compared to 16.2 ± 2.8 ppm/g wet soil in the original permafrost (Fig. 5). Mackelprang et al. (2011) observed a burst of methane release from the permafrost within 2 days of thaw and showed that the rapid release of methane mainly originated from the gas trapped in the permafrost before it thawed, and that much of the methane was subsequently consumed by methanotrophic bacteria. Despite the incubation time, the methanogenic activity was thought to play an important role for mass of methane emission. McCalley et al. (2014) used $\delta^{13}C$ signature to reveal that methane emission was regulated by microbial activities in response to permafrost thaw. Microbial decomposition of organic matter is thought to be the dominant pathway of carbon return from terrestrial ecosystems to the atmosphere (Schuur et al. 2008).

As permafrost thaws, many changes in ecosystems will be triggered, including those involving physicochemical properties and functions. Permafrost thaw can substantially change the surface hydrology. In ice-rich and poorly drained permafrost, collapse-scar bogs and thermokarst lakes were often developed (Jansson and Tas 2014), and in well-drained upland boreal soils, permafrost thaw often leads to increased rates of evapotranspiration and ultimately results in soil drying (Allison and Treseder 2011). In the past few decades, the Qinghai–Tibetan Plateau was also subjected to permafrost thaw due to climate warming. The thawed bogs and thermokarst ponds or rivers are often observed in our sampling sites (Fig. 6). It is well known that permafrost thaw will increase the active layer thickness and lead to the stored organic carbon in the permafrost being released into the active layer for microbial decomposition. Our data showed that the acetate content which had accumulated in the thawed permafrost made the soil pH lower than that in the original permafrost during the short-term incubation time. The accumulated acetate was due to the activities of acetogenic bacteria (Coolen and Orsi 2015). We inferred that the acidic soil pH may affect the availability of nutrients to plants and activity of soil microorganisms in the long-term. Soil texture refers to the relative amounts of sand, silt, and clay in a soil, which is an important soil characteristic and has a profound effect on the properties of soils, such as water holding capacity, nutrient retention and supply, drainage, and nutrient leaching. Our data showed that the soil textures, whether before or after the thawing of the permafrost, were all classified as clay. However, the percentage of sand particles was reduced slightly from 25.63% in the original permafrost to 23.67% in the thawed permafrost, which was attributed to the biogenic acidic weathering. As weathering continues, the soil particles shift from sand to silt and clay, which in turn, will increase both the soil water and nutrient holding capacity, but may also cause insufficient soil aeration. Mineral composition analysis showed that the percentage of dolomite was reduced, which was caused by the bioweathering process. It is known that weathering is the principal process that acts upon the Earth's primary minerals to form soil. As soil particles begin to weather, primary minerals initially release nutrients into the soil. However, because these particles are continuously being weathered, the capacity to hold and retain nutrients is greatly reduced, leading to most nutrients being lost to leaching. These changes, in the long-term, can significantly influence succession in permafrost ecosystems.

Acknowledgements The authors acknowledge James Hurley at the University of Colorado for making a critical reading and revision of this paper. This research was supported by Funds of Oil and Gas Survey, China Geological Survey (GZH201400308 and GZH201400306).

References

Allison SD, Treseder KK (2011) Climate changes feedbacks to microbial decomposition in boreal soils. Fungal Ecol 4:362–374

Anisimov OA, Nelson FE (1996) Permafrost distribution in the Northern Hemisphere under scenarios of climatic change. Glob Planet Change 14:59–72

Anthony KMW, Zimov SA, Grosse G, Jones MC, Anthony PM, Chapin FS III, Finlay JC, Mack MC, Davydov S, Frenzel P, Frolking S (2014) A shift of thermokarst lakes from carbon sources to sinks during the Holocene epoch. Nature 511:452–456

Barbier BA, Dziduch I, Liebner S, Ganzert L, Lantuit H, Pollard W, Wagner D (2012) Methane cycling communities in a permafrost-affected soil on Herschel Island, Western Canadian Arctic: active layer profiling of *mcrA* and *pmoA* genes. FEMS Microbiol Ecol 82:287–302

Chapin FS III, Sturm M, Serreze MC, McFadden JP, Key JR, Lloyd AH et al (2005) Role of land-surface changes in Arctic summer warming. Science 310:657–660

Christensen TR, Johansson T, Åkerman HJ, Mastepanov M (2004) Thawing sub-arctic permafrost: effects on vegetation and methane emissions. Geophys Res Lett 31:1–4

Conrad R, Erkel C, Liesack W (2006) Rice Cluster I methanogens, an important group of *Archaea* producing greenhouse gas in soil. Curr Opin Biotech 17:262–267

Coolen MJL, Orsi WD (2015) The transcriptional response of microbial communities in thawing Alaskan permafrost soils. Front Microbiol 6:1–14

Coolen MJL, van de Giessen J, Zhu EY, Wuchter C (2011) Bioavailability of soil organic matter and microbial community dynamics upon permafrost thaw. Environ Microbiol 13:2299–2314

DeLong EF (1992) Archaea in coastal marine environments. PNAS 89:5685–5689

Deng J, Gu Y, Zhang J, Xue K, Qin Y, Yuan M, Yin H, He Z, Wu L, Schuur EAG, Tiedje JM, Zhou J (2015) Shifts of tundra bacterial and archaeal communities along a permafrost thaw gradient in Alaska. Mol Ecol 24:222–234

Ernakovich JG, Wallenstein MD (2015) Permafrost microbial community traits and functional diversity indicate low activity at in situ thaw temperatures. Soil Biol Biochem 87:78–89

Garcia JL, Ollivier B, Whitman WB (2006) The order Methanomicrobiales. Prokaryotes 3:208–230

Good IJ (1953) The population frequencies of species and estimation of population parameters. Biometrika 40:237–264

Graham DE, Wallenstein MD, Vishnivetskaya TA, Waldrop MP, Phelps TJ, Pfiffner SM et al (2012) Microbes in thawing permafrost: the unknown variable in the climate change equation. ISME J 6:709–712

Grosskopf R, Stubner S, Liesack W (1998) Novel euryarchaeotal lineages detected on rice roots and in the anoxic bulk soil of flooded rice microcosms. Appl Environ Microbiol 64:4983–4989

Hales BA, Edwards C, Ritchie DA, Hall G, Pickup RW, Saunders JR (1996) Isolation and identification of methanogen-specific DNA from blanket bog peat by PCR amplification and sequence analysis. Appl Environ Microbiol 62:668–675

Hallam SJ, Girguis PR, Preston CM, Richardson PM, DeLong EF (2003) Indentification of methyl coenzyme M reductase A (*mcrA*) genes associated with methane-oxidizing archaea. Appl Environ Microbiol 69:5483–5491

Hultman J, Waldrop MP, Mackelprang R, David MM, McFarland J, Blazewicz SJ et al (2015) Multi-omics of permafrost, active layer and thermokarst bog soil microbiomes. Nature 521:208–212

Jansson JK, Tas N (2014) The microbial ecology of permafrost. Nat Rev Microbiol 12:414–425

Jin H, Wu J, Cheng G, Tomoko N, Sun G (1999) Methane emissions from wetlands on the Qinghai–Tibet Plateau. Chin Sci Bull 44:2282–2286

Jin HJ, Li SX, Wang SL, Zhao L (2000) Impact of climatic change on permafrost and cold regions environment in China. Acta Geogr Sin 55:161–173

Kang X (1996) The features of climate change in the Qinghai–Tibetan Plateau region in the past 40 years. J Glaciol Geocryol 18(Suppl. 1):281–288

Kendall MM, Boone AD (2006) The order Methanosarciales. Prokaryotes 3:244–256

Lawrence DM, Slater AG (2005) A projection of severe near-surface permafrost degradation during the 21st century. Geophys Res Lett 32:1–5

Liebner S, Ganzert L, Kiss A, Yang S, Wagner D, Svenning MM (2015) Shifts in methanogenic community composition and methane fluxes along the degradation of discontinuous permafrost. Front Microbiol 6:1–10

Luton PE, Wayne JM, Sharp RJ, Riley PW (2002) The *mcrA* gene as an alternative to 16S rRNA in the phylogenetic analysis of methanogen population in landfill. Microbiology 148:3521–3530

Mackelprang R, Waldrop MP, DeAngelis KM, David MM, Chavarria KL, Blazewicz SJ, Rubin EM, Jansson JK (2011) Metagenomic analysis of a permafrost microbial community reveals a rapid response to thaw. Nature 2011:368–371

McCalley CK, Woodcroroft BJ, Hodgkins SB, Wehr RA, Kim EH, Mondav R, Crill PM, Chanton JP, Rich VI, Tyson GW, Saleska SR (2014) Methane dynamics regulated by microbial community response to permafrost thaw. Nature 514:478–481

McGuire AD, Anderson LG, Christensen TR, Dallimore S, Guo L, Hayes DL, Heimann M, Lorenson TD, Macdonald RW, Roulet N (2009) Sensitivity of the carbon cycle in the Arctic to climate change. Ecol Monogr 79:523–555

Meng J, Xu J, Qin D, He Y, Xiao X, Wang F (2014) Genetic and functional properties of uncultivated MCG archaea assessed by metagenome and gene expression analysis. ISME J 8:650–659

Metje M, Frenzel P (2005) Effect of temperature on anaerobic ethanol oxidation and methanogenesis in acidic peat from a northern wetland. Appl Environ Microbiol 71:8191–8200

Mondav R, Woodcroft B, Kim EH, McCalley CK, Hodgkins SB, Crill PM et al (2014) Discovery of a novel methanogen prevalent in thawing permafrost. Nat Commun 5:3212

Nunoura T, Oida H, Miyazaki J, Miyashita A, Imachi H, Takai K (2008) Quantification of *mcrA* by fluorescent PCR in methanogenic and methanotrophic microbial communities. FEMS Microbiol Ecol 64:240–247

Ochsenreiter T, Selezi D, Quaiser A, Bonch-Osmolovskaya L, Schleper C (2003) Diversity and abundance of *Crenarchaeota* in terrestrial habitats studied by 16S RNA surveys and real time PCR. Environ Microbiol 5:787–797

Osterkamp TE, Viereck L, Shur Y, Jorgensons MT, Racine C, Doyle A, Boone RD (2000) Observations of thermokarst and its impact on boreal forests in Alaska, USA. Arct Antarct Alp Res 32:303–315

Rivkina E, Shcherbakova V, Laurinavichius K, Petrovskaya L, Krivushin K, Kraev G, Pecheritsina S, Gilichinsky D (2007) Biogeochemistry of methane and methanogenic archaea in permafrost. FEMS Microbiol Ecol 61:1–15

Sakai S, Imachi H, Hanada S, Ohashi A, Harada H, Kamagata Y (2008) *Methanocella paludicola* gen. nov., sp. nov., a methane-producing archaeon, the first isolate of the lineage 'Rice Cluster I', and proposal of the new archaeal order *Methanocellales* ord. nov. Int J Syst Evol Microbiol 58:926–936

Schloss PD, Handelsman J (2005) Introducing DOTUR, a computer program for defining operational taxonomic units and estimating species richness. Appl Environ Microbiol 71:1501–1506

Schloss PD, Westcott SI, Ryabin T, Hall JR, Hartmann M, Hollister EB et al (2009) Introducing mothur: open-source, platform-independent, community-supported software for describing and comparing microbial communities. Appl Environ Microbiol 75:7537–7541

Schuur EAG, Bockheim J, Canadell JG, Euskirchen E, Field CB, Goryachkin SV et al (2008) Vulnerability of permafrost carbon to climate change: implications for the global carbon cycle. Bioscience 58:701–714

Schuur EAG, Vogel JG, Crummer KG, Lee H, Sickman JO, Osterkamp TE (2009) The effect of permafrost thaw on old carbon release and net carbon exchange from tundra. Nature 459:556–559

Smith LC, MacDonald GM, Velichko AA, Beilman WD, Borisova OK, Frey KE, Kremenetski KV, Sheng Y (2004) Siberian peatlands: a net carbon sink and global methane source since the early Holocene. Science 303:353–356

Steven B, Leveille R, Pollard WH, Whyte LG (2006) Microbial ecology and biodiversity in permafrost. Extremophiles 10:259–267

Steven B, Wayne HP, Charles WG, Lyle GW (2008) Microbial diversity and activity through a permafrost/ground ice core profile from the Canadian high Arctic. Environ Microbiol 10:3388–3403

Sturn M, Racine C, Tape K (2001) Climate change: increasing shrub abundance in the Arctic. Nature 411:546–547

Takai K, Horikoshi K (2000) Rapid detection and quantification of members of the archaeal community by quantitative PCR using fluorogenic probes. Appl Environ Microbiol 66:5066–5072

Vitt DH, Halsey LA, Zoltai SC (2000) The changing landscape of Canada's western boreal forest: the current dynamics of permafrost. Can J For Res 30:283–287

Wagner D (2008) Microbial communities and processes in Arctic permafrost environments. In: Dion P, Nautiyal CS (eds) Microbiology of extreme soils. Springer, Berlin, pp 133–154

Wagner D, Kobabe S, Pfeiffer EM, Hubberten HW (2003) Microbial controls on methane fluxes from a polygonal tundra of the Lena Delta, Siberia. Permafr Periglac 14:173–185

Wang G, Qian J, Cheng G, Lai Y (2002) Soil organic carbon pool of grassland soils on the Qinghai–Tibetan Plateau and its global implication. Sci Total Environ 291:207–217

Wang P, Huang X, Pang S, Zhu Y, Lu Z, Zhuang S, Liu H, Yang K, Li B (2014) Geochemical dynamics of the gas hydrate system in the Qilian Mountain permafrost, Qinghai, Northwest China. Mar Petrol Geol 59:72–90

Wei S, Cui H, He H, Hu F, Su X, Zhu Y (2014) Diversity and distribution of Archaea community along a stratigraphic permafrost profile from Qinghai–Tibetan Plateau, China. Archaea 2014. (**Article ID240817**)

Woo MK (1992) Impacts of climatic variability and change on Canadian wetlands. Can Water Resour J 17:63–69

Yang M, Nelson FE, Shiklomanov NI, Guo D, Wan G (2010a) Permafrost degradation and its environmental effects on the Tibetan Plateau: a review of recent research. Earth Sci Rev 103:31–44

Yang ZP, Ou YH, Xu XL, Zhao L, Song MH, Zhou CP (2010b) Effects of permafrost degradation on ecosystem. Acta Ecol Sin 30:33–39

Zhang T, Barry RG, Knowles K, Heginbottom JA, Brown J (1999) Statistic and characteristics of permafrost and ground-ice distribution in the Northern Hemisphere. Polar Geogr 23:132–154

Zimov SA, Schuur EAG, Chapin FS (2006) Permafrost and the global carbon budget. Science 312:1612–1613